Tunable Fe^{2+}:ZnSe passively Q-switched Ho^{3+}-doped ZBLAN fiber laser around 3 μm

Jianfeng Li,[1,2,*] Hongyu Luo,[1] Lele Wang,[1] Bo Zhai,[1] Heping Li,[1] and Yong Liu[1]

[1]*State Key Laboratory of Electronic Thin Films and Integrated Devices, School of Optoelectronic Information, University of Electronic Science and Technology of China (UESTC), Chengdu 610054, China*
[2]*Suzhou Institute of Biomedical Engineering and Technology, Chinese Academy of Sciences, Suzhou 215163, China*
[*]*lijianfeng@uestc.edu.cn*

Abstract: We report a tunable passively Q-switched Ho^{3+}-doped ZBLAN fiber laser at 3 μm waveband using a Fe^{2+}:ZnSe crystal as saturable absorber (SA) and a plane ruled grating in Littrow configuration as wavelength tuning element. Stable pulse trains with ~85 nm tuning range from 2919.1 nm to 3004.2 nm and spectrum bandwidths of ~1 nm were achieved for the Fe^{2+}:ZnSe crystal with an initial transmission (IT) of 69%. Pulse duration increased from 1.23 μs to 2.35 μs and repetition rate decreased from 96.1 kHz to 43.56 kHz with the extension towards long wavelength direction. With the IT increasing to 79% and then 89%, though the available tuning range was slightly shortened, higher output power, pulse energy and slope efficiency were obtained with the slightly increased pulse duration and repetition rate. Maximum output power of 337 mW at a slope efficiency of 11.44% and pulse energy of 5.64 μJ were achieved at ~2970 nm and ~2991 nm, respectively. High signal noise ratio (SNR) of over 50 dB across the whole tuning range for the three ITs Fe^{2+}:ZnSe crystals indicated the stable Q-switching. To our knowledge, this is the first reported wavelength tunable passively Q-switched ZBLAN fiber laser.

OCIS codes: (140.3510) Lasers, fiber; (140.3480) Lasers, diode-pumped.

References and links

1. S. D. Jackson, "Towards high-power mid-infrared emission from a fibre laser," Nat. Photonics **6**(7), 423–431 (2012).
2. I. T. Sorokina and K. L. Vodopyanov, *Solid-state Mid-infrared Laser Sources* (Springer, 2003).
3. S. D. Jackson and T. King, "High-power diode-cladding-pumped Tm-doped silica fiber laser," Opt. Lett. **23**(18), 1462–1464 (1998).
4. R. Allen and L. Esterowitz, "CW diode pumped 2.3 μm fiber laser," Appl. Phys. Lett. **55**(8), 721–722 (1989).
5. R. Li, J. Li, L. Shterengas, and S. D. Jackson, "Highly efficient holmium fiber laser diode pumped at 1.94 μm," Electron. Lett. **47**(19), 1089–1090 (2011).
6. S. D. Jackson, "Single-transverse-mode 2.5-W holmium-doped fluoride fiber laser operating at 2.86 μm," Opt. Lett. **29**(4), 334–336 (2004).
7. J. Li, D. D. Hudson, and S. D. Jackson, "High-power diode-pumped fiber laser operating at 3 μm," Opt. Lett. **36**(18), 3642–3644 (2011).
8. C. Carbonnier, H. Tobben, and U. B. Unrau, "Room temperature CW fibre laser at 3.22 μm," Electron. Lett. **34**(9), 893–894 (1998).
9. J. Schneider, C. Carbonnier, and U. B. Unrau, "Characterization of a Ho^{3+}-doped fluoride fiber laser with a 3.9-μm emission wavelength," Appl. Opt. **36**(33), 8595–8600 (1997).
10. S. D. Jackson, M. Pollnau, and J. F. Li, "Diode pumped erbium cascade fiber laser," IEEE J. Quantum Electron. **47**(4), 471–478 (2011).
11. O. Henderson-Sapir, J. Munch, and D. J. Ottaway, "Mid-infrared fiber lasers at and beyond 3.5 μm using dual-wavelength pumping," Opt. Lett. **39**(3), 493–496 (2014).
12. S. D. Jackson, "Continuous wave 2.9 μm dysprosium-doped fluoride fiber laser," Appl. Phys. Lett. **83**(7), 1316–1318 (2003).
13. S. Tokita, M. Murakami, S. Shimizu, M. Hashida, and S. Sakabe, "12 W Q-switched Er:ZBLAN fiber laser at 2.8 μm," Opt. Lett. **36**(15), 2812–2814 (2011).

#241509 Received 21 May 2015; revised 17 Jul 2015; accepted 29 Jul 2015; published 17 Aug 2015

14. J. Li, T. Hu, and S. D. Jackson, "Dual wavelength Q-switched cascade laser," Opt. Lett. **37**(12), 2208–2210 (2012).
15. J. Li, T. Hu, and S. D. Jackson, "Q-switched induced gain switching of a two-transition cascade laser," Opt. Express **20**(12), 13123–13128 (2012).
16. T. Hu, D. D. Hudson, and S. D. Jackson, "Actively Q-switched 2.9 μm $Ho^{3+}Pr^{3+}$-doped fluoride fiber laser," Opt. Lett. **37**(11), 2145–2147 (2012).
17. J. Li, Y. Yang, D. D. Hudson, Y. Liu, and S. D. Jackson, "A tunable Q-switched Ho3+-doped fluoride fiber laser," Laser Phys. Lett. **10**(4), 045107 (2013).
18. C. Wei, X. Zhu, F. Wang, Y. Xu, K. Balakrishnan, F. Song, R. A. Norwood, and N. Peyghambarian, "Graphene Q-switched 2.78 μm Er^{3+}-doped fluoride fiber laser," Opt. Lett. **38**(17), 3233–3236 (2013).
19. J. Li, H. Luo, Y. He, Y. Liu, L. Zhang, K. Zhou, A. G. Rozhin, and S. K. Turistyn, "Semiconductor saturable absorber mirror passively Q-switched 2.97 μm fluoride fiber laser," Laser Phys. Lett. **11**(6), 065102 (2014).
20. C. Wei, X. Zhu, R. A. Norwood, and N. Peyghambarian, "Passively Q-Switched 2.8 μm Nanosecond Fiber Laser," IEEE Photonics Technol. Lett. **24**(19), 1741–1744 (2012).
21. G. Zhu, X. Zhu, K. Balakrishnan, R. A. Norwood, and N. Peyghambarian, "Fe^{2+}:ZnSe and graphene Q-switched singly Ho^{3+}-doped ZBLAN fiber lasers at 3 μm," Opt. Mater. Express **3**(9), 1365–1377 (2013).
22. J. Liu, S. Wu, Q. H. Yang, and P. Wang, "Stable nanosecond pulse generation from a graphene-based passively *Q*-switched Yb-doped fiber laser," Opt. Lett. **36**(20), 4008–4010 (2011).
23. Z. Luo, M. Zhou, J. Weng, G. Huang, H. Xu, C. Ye, and Z. Cai, "Graphene-based passively Q-switched dual-wavelength erbium-doped fiber laser," Opt. Lett. **35**(21), 3709–3711 (2010).
24. J. Liu, J. Xu, and P. Wang, "Graphene-based passively Q-switched 2 μm thulium-doped fiber laser," Opt. Commun. **285**(24), 5319–5322 (2012).
25. A. A. Voronov, V. I. Kozlovskii, Y. V. Korostelin, A. I. Landman, Y. P. Podmarkov, V. G. Polushkin, and M. P. Frolov, "Passive Fe^{2+}:ZnSe single-crystal Q switch for 3-μm lasers," Quantum Electron. **36**(1), 1–2 (2006).
26. A. Gallian, A. Martinez, P. Marine, V. Fedorov, S. Mirov, V. Badikov, D. Boutoussov, and M. Andriasyan, "Fe:ZnSe passive Q-switching of 2.8-μm Er:Cr:YSGG laser Cavity," Proc. SPIE **6451**(64510L), 64510L (2007).
27. B. Braun, F. X. Kärtner, G. Zhang, M. Moser, and U. Keller, "56-ps passively Q-switched diode-pumped microchip laser," Opt. Lett. **22**(6), 381–383 (1997).
28. Z. Yu, Y. Song, J. Tian, Z. Dou, H. Guoyu, K. Li, H. Li, and X. Zhang, "High-repetition-rate Q-switched fiber laser with high quality topological insulator Bi_2Se_3 film," Opt. Express **22**(10), 11508–11515 (2014).
29. C. Hönninger, R. Paschotta, F. Morier-Genoud, M. Moser, and U. Keller, "Q-switching stability limits of continuous-wave passive mode locking," J. Opt. Soc. Am. B **16**(1), 46–56 (1999).

1. Introduction

Mid-infrared (mid-IR) lasers have attracted a great deal of attention owing to their wide range of applications in such as medical diagnosis, chemical bond spectroscopy, gas sensing, missile countermeasures, and nonlinear mid-infrared photonics [1]. Various technologies have been exploited to produce mid-IR laser including quantum cascade lasers (QCLs), solid state lasers, difference frequency generation (DFG), sum frequency generation (SFG), optical parametric oscillator (OPO), etc [2]. With the development of infrared glass fiber, mid-IR fiber lasers has become a promising area of research, because of their unique advantages such as excellent beam quality, good heat dissipation, high efficiency and flexible design. Until recently the research in mid-IR fiber lasers has been mainly focused at waveband of 2~4 μm by employing Tm^{3+} (producing gain around 2.0 and 2.3 μm) [3, 4], Ho^{3+} (producing gain at about 2.1, 2.8, 3.0, 3.2, and 3.9 μm) [5–9], Er^{3+} (producing gain at 2.9 and 3.5 μm) [10, 11] and Dy^{3+} (producing gain at 2.9 μm) [12] doped ZBLAN fibers.

Compared to CW and mode-locked fiber lasers, Q-switched fiber lasers especially with tunable wavelength at 3 μm waveband can offer energetic and flexible pulses with ns or ms pulse duration that are desirable in some special applications such as gas sensing, plastic and polymer processing, laser scalpel, non-invasive medical diagnosis, infrared countermeasures and laser radar. Currently, the reported ~3 μm mid-IR Q-switched fiber lasers can be roughly divided into two major categories. The first one is active Q-switching where the acousto-optic modulator (AOM) is employed inside the cavity [13–17]. A 2.8 μm actively Q-switched Er^{3+}-doped ZBLAN fiber laser with pulse duration of 90 ns and power of 10 W has been recently demonstrated [13]. Using a piece of singly Ho^{3+}-doped ZBLAN fiber, we have achieved active Q-switching at 3.002 μm with pulse duration of 260 ns [14]. Also T. Hu *et.al* demonstrated an actively Q-switched Ho^{3+}/Pr^{3+} co-doped ZBLAN fiber laser operating at 2.86 μm with pulse duration of 70 ns [16]. More recently, we have presented the wavelength

#241509 Received 21 May 2015; revised 17 Jul 2015; accepted 29 Jul 2015; published 17 Aug 2015

tunability of actively Q-switched Ho^{3+}-doped ZBLAN fiber laser by using an Au-coated plane ruled grating [17]. The second one is passive Q-switching in which the compact saturable absorber (SA) such as graphene, Fe^{2+}:ZnSe crystal and semiconductor saturable absorber mirror (SESAM) is introduced into the cavity instead of the externally driven modulators [18–21]. This technique exhibits the advantages of compact structure and low cost compared to the active Q-switching. Graphene, as a novel kind of two-dimensional (2D) Dirac material, possesses a prominent broadband saturable absorption property owing to its zero bandgap structure and has been widely applied in Q-switching fiber lasers at 1 μm [22], 1.55 μm [23] and 2 μm [24] bands. Recently, a 2.78 μm graphene-based Q-switched pulsed Er^{3+}-doped ZBLAN fiber laser with pulse duration of 2.9 μs and pulse energy of 1.67 μJ has been demonstrated [18]. However, relatively low damage threshold and modulation depth of graphene are not suited to achieving high energy Q-switched pulses. SESAM, as a type of mature commercial saturable absorber, has not only a remarkably excellent performance but also the ability of customizing some of its parameters e.g., modulation depth, non-saturable loss, recovery time, etc. However, the distributed Bragg reflector (DBR) in SESAM requires increased reflection layers for the long operation wavelength hence improving the cost and complicating the fabrication. For example, the DBR operating at 3 μm needs 25 layer AlAs/GaAs pairs with a thickness of 12 μm and 24 hours fabrication process at a growth rate of 0.5 μm/h. Very recently, we have presented a passively Q-switched Ho^{3+}-doped ZBLAN fiber laser at 2.97 μm using a specifically designed broadband SESAM [19]. In this SESAM, an InAs absorber layer was sandwiched between an Au-coated mirror and a GaAs wafer to improve the operation band and damage threshold [19]. Furthermore, Fe^{2+}:ZnSe crystal as a result of its high damage threshold (~2 J/cm^2), large absorption cross-section and small saturation fluence has been also widely applied in high energy mid-IR Q-switching of especially solid-state lasers [25, 26]. As the transmission type SA, it is also very suitable for the pulsed fiber lasers with the ring cavity or linear cavity involving some specific cavity terminators such as FBG, CFBG, bulk grating. Recently, based on Fe^{2+}:ZnSe crystal SA, a passively Q-switched 2.8 μm Er^{3+}-doped ZBLAN fiber laser with pulse duration of 370 ns and pulse energy of 2.0 μJ [20] and 2.93 μm Ho^{3+}-doped ZBLAN fiber laser with pulse duration of 0.82 μs and pulse energy of 460 nJ have been demonstrated [21].

In this paper, we report for the first time a tunable passively Q-switched ZBLAN fiber laser with the tuning range from 2919.1 nm to 3004.2 nm using a Fe^{2+}:ZnSe crystal as the SA and a plane ruled grating as the wavelength tuning element. The performances e.g., pulse duration, repetition rate, output power, pulse energy and slope efficiency of this fiber laser were also investigated when tuning the wavelength and varying the initial transmission (IT) of the Fe^{2+}:ZnSe crystal. The revealed rules are quite critical for designing the passively Q-switched fiber lasers in this wavelength region.

2. Experiment setup and results

The schematic diagram of the tunable passively Q-switched Ho^{3+}-doped ZBLAN fiber laser using Fe^{2+}:ZnSe crystal as the SA is shown in Fig. 1. Here, the laser from two commercially available high power 1150 nm diode lasers (Eagleyard Photonics) was coupled into the gain fiber by polarization multiplexing via a polarized beam splitter (PBS) (Thorlabs) and focusing using an anti-reflection coated ZnSe objective lens (Innovation Photonics, LFO-5-6-0.975/3 μm, 0.25 NA) with a 6.0 mm focal length acting as the collimator for light out-coupled from the fiber core as well. A dichroic mirror (Thorlabs, 96%T@1150 nm, 95%T@ ~3 μm) was placed between the PBS and the ZnSe objective lens at an angle of 45° with respect to pump beam to output the laser emission. Afterwards a 3 μm filter with FWHM of 500 nm (Throlabs) was used to block the residual pump. The gain fiber was a piece of double-clad ZBLAN fiber (Fiberlabs) whose pump cladding is D-shaped with a diameter of 125 μm and a numerical aperture (NA), core has a diameter of 10 μm and a NA of 0.2. Herein, the Ho^{3+} ions dopant concentration was 1.5 mol.%. Employing the typical cutback method, the launch

#241509 Received 21 May 2015; revised 17 Jul 2015; accepted 29 Jul 2015; published 17 Aug 2015

efficiency and fiber absorption coefficient were measured to be 80% and 0.36 m^{-1}, respectively. Thus the selected 7.0 m fiber could provide 92% pump absorption efficiency. One fiber end was perpendicularly cleaved acting as output coupler with the aid of 4% Fresnel reflection. The other fiber end was cleaved at an angle of 8° to avoid the parasitic lasing. The light from the angle cleaved end was collimated via an anti-reflection coated ZnSe objective lens and finally terminated by a Au-coated plane ruled grating (Thorlabs, 300 lines per mm, blaze wavelength λ_B = 3 μm, blaze angle θ_B = 26.7°) with a distance of 50 cm from the angle cleaved fiber end, which was used to provide the feedback while tuning the laser transition. A confocal scheme consisting of two same plano-covex CaF_2 lens (Thorlabs LA5370) with focal length of 40 mm was inserted between the ZnSe objective lens and the grating along the light path. A cube polycrystalline Fe^{2+}:ZnSe crystal with 6.7 mm length, 6.7 mm width and 1.6 mm thickness (IPG photonics) as shown in the inset of Fig. 1 acting as the SA was placed at the focus of the confocal scheme to maximize the influence. Three Fe^{2+}:ZnSe crystals with ITs of ~69%, ~79% and ~89% at 3.0 μm waveband were used respectively in the experiment. Note that they were all coated with anti-reflection films at 1~5 μm. An InAs detector with a response time of 2 ns driven by an in-house designed circuit was employed and connected with a 500 MHz bandwidth digital oscilloscope to record the pulse temporal waveform. An RF spectrum analyzer (Advantest R3267) with resolution bandwidth of 10 Hz to 100 MHz was utilized to measure the signal-to-noise ratio (SNR) of pulses. A monochromator with scanning resolution of 0.1 nm (Princeton instrument Acton SP2300) was employed to measure the laser spectrum.

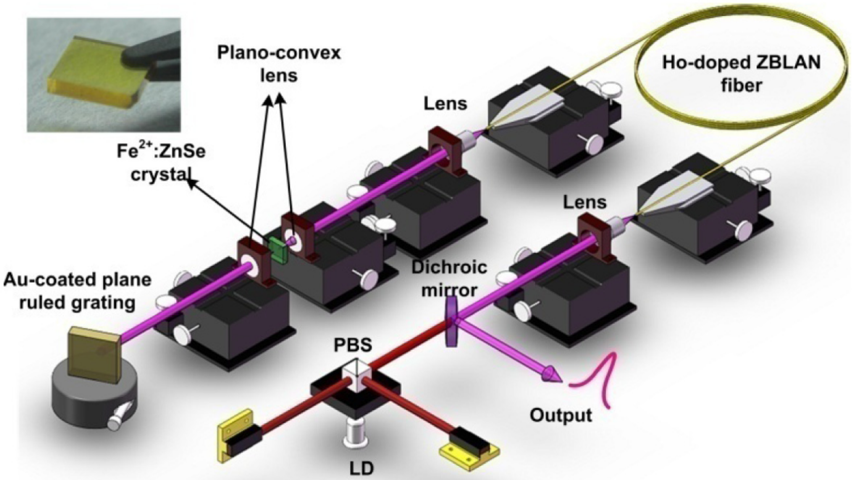

Fig. 1. Experimental setup of tunable passively Q-switched Ho^{3+}-doped ZBLAN fiber laser based on Fe^{2+}:ZnSe crystal SA. Inset: Photograph of Fe^{2+}:ZnSe crystal sample.

Firstly, the Fe^{2+}:ZnSe crystal with IT of 69% was employed and the grating was adjusted to maximize the output power. The oscillator started to operate at continuous wave (CW) regime at the launched pump power of 0.506 W. Then, stable Q-switched pulses were observed as the launched pump power was increased to 0.664 W and the Q-switching could be maintained to maximum pump power of 3.32 W. The typical pulse train and envelop of single pulse were shown in Fig. 2(a). The pulse duration and repetition rate were measured to be 1.92 μs and 62.74 kHz, respectively. The right inset of Fig. 2(a) shows the RF spectrum of the output at a scanning range of 45 kHz with a resolution of 100 Hz. The high SNR of 51 dB indicates the laser operated at stable Q-switching regime. Figure 2(b) shows the output power, pulse energy, repetition rate, duration and peak power as a function of the launched pump power. Here, the pulse energy and peak power were estimated according to their

#241509 Received 21 May 2015; revised 17 Jul 2015; accepted 29 Jul 2015; published 17 Aug 2015

corresponding output power, repetition rate and pulse duration owing to the high SNR. It is observed that the repetition rate increases from 24.83 kHz to 62.74 kHz and the pulse duration decrease from 5.05 μs to 1.92 μs, respectively as the pump power is increased from 0.664 W to 3.32 W, resulting from the faster population built-up and higher energy storage on $^5I_6$ level. No pulse duration saturation even at the maximum pump power was observed indicating the SA at this pump level was not fully bleached. Maximum output power of 266 mW was achieved at a slope efficiency of 9.02% corresponding to the pulse energy of 4.24 μJ, which were only limited by the available pump power.

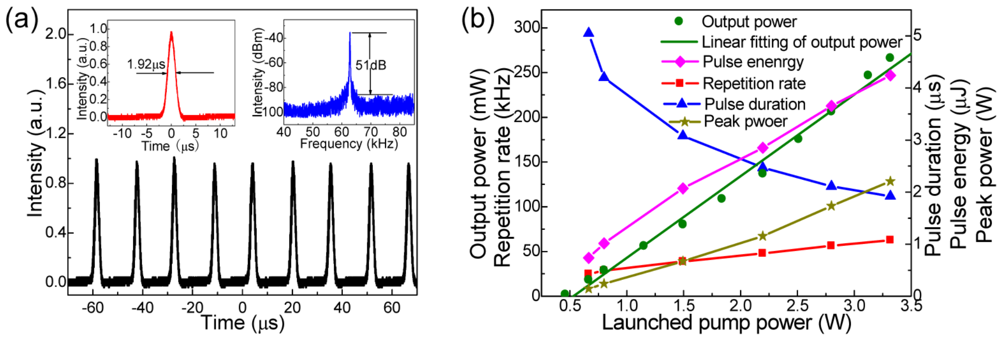

Fig. 2. (a) Temporal domain pulse train at the launched pump power of 3.32 W using 69% IT Fe^{2+}:ZnSe crystal SA. Inset: single pulse profile at a 26 μs scanning range and RF spectrum at a scanning range of 45 kHz. (b) Measured output power, repetition rate, pulse duration and calculated pulse energy and peak power as a function of the launched pump power.

Then the laser transition was tuned by rotating the platform holding the plane ruled grating from 45′ in clockwise direction to 43′ in anticlockwise direction with respect to the position of delivering maximum output power. Figure 3(a) shows the optical spectra of Q-switched pulses at the maximum launched pump power of 3.32 W. Tuning range of ~85 nm spanning from 2919.1 nm to 3004.3 nm with a linewidth of ~1.0 nm over the entire tuning range was gained. In our experiment, the wavelength tuning resolution was mainly limited by the used rotating platform whose adjustment resolution was 2′. Therefore, the average tuning resolution under full-power operation was calculated to be ~2 nm. Note that the spectrum profiles of tuned wavelengths shown in a linear scale were all normalized for their visibilities. Further rotating the grating, once beyond the tuning edges, the stable Q-switching was ceased and changed to the CW operation with a suddenly varied wavelength of 2976.0 nm and substantially broadened FWHM bandwidth of 11.5 nm, as shown in Fig. 3(b). This is due to the sharply reduced gain outside of the tuning range leading to the failed competition with CW oscillation. In this case, the back feedback of CW oscillation came from the residual Fresnel reflection of the plano-convex CaF_2 lens close to the perpendicularly cleaved fiber end.

#241509 Received 21 May 2015; revised 17 Jul 2015; accepted 29 Jul 2015; published 17 Aug 2015

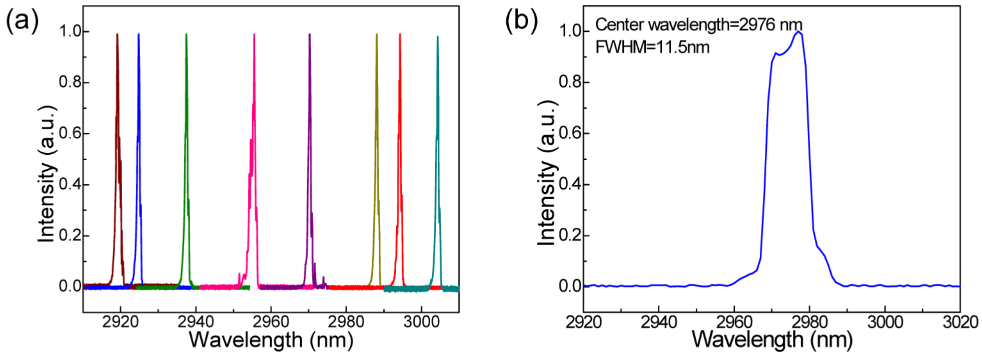

Fig. 3. (a) Measured output spectrum as tuning the $^5I_6 \rightarrow ^5I_7$ transition at the maximum launched pump power of 3.32 W. (b) Measured output power once the grating beyond tuning edge.

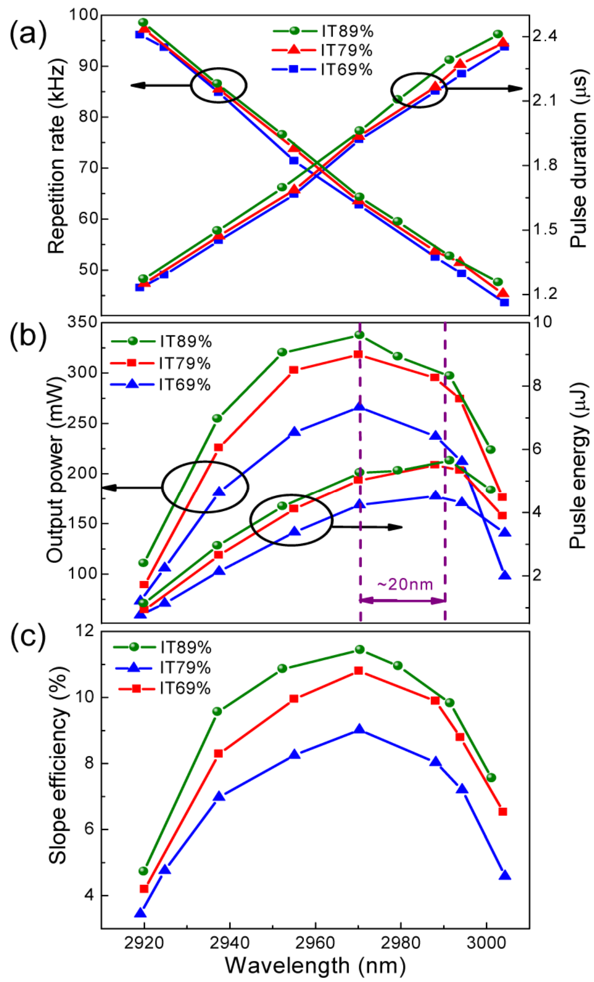

Fig. 4. (a) Repetition rates and pulse durations, (b) output powers and pulse energies and (c) slope efficiencies as a function of tuning wavelength when employing 69%, 79%, 89% IT Fe^{2+}:ZnSe crystals as the SA, respectively at the maximum launched pump power of 3.32 W.

Afterwards, either 79% or 89% IT Fe^{2+}:ZnSe crystal was employed to replace the previous 69% IT one. Similar stable Q-switched pulses were observed for both 79% and 89% IT

#241509 Received 21 May 2015; revised 17 Jul 2015; accepted 29 Jul 2015; published 17 Aug 2015

Fe^{2+}:ZnSe crystals only with slightly shortened tuning ranges of 2920.1~3003.9 nm and 2919.9~3001.2 nm, respectively. It was because that higher intra-cavity gain was required to maintain the Q-switching for higher IT. Figure 4(a) shows the repetition rate and pulse duration as a function of the tuning wavelength using the Fe^{2+}:ZnSe SAs with ITs of 69%, 79% and 89%, respectively, at the maximum launched pump power of 3.32 W. It is observed that the repetition rate decreases and the pulse duration increases near-linearly for all the three IT SAs as tuning towards long wavelength direction. This is resulted from the combined function of changes of gain, threshold, dispersion and modulation depth of SA with the varied wavelength. Moreover, slightly higher repetition rate is observed for higher IT as a result of the decreased threshold thus shortening the time for inversion population to arrive at the threshold level. On the other hand, the pulse duration also slightly increases with IT considering the fact that lower threshold leads to the decrease of accumulated population density on upper laser level thus longer time for generating a Q-switched pulse is required. Finally, the shortest pulse duration of 1.23 μs at the tuning edge of 2919.1 nm was achieved using 69% IT SA, while the maximum repetition rate of 98.5 kHz was obtained using the 89% IT SA at its tuning edge of 2919.9 nm. Figure 4(b) shows the output powers and pulse energies with respect to ITs of 69%, 79%, 89% as a function of tuning wavelength at the maximum pump power. It can be seen that for the three SAs with different ITs, both output power and pulse energy increase initially and then decrease with wavelength, well matching with the intra-cavity gain profile. However, we can see an about 20 nm gap between the peak positions of output power and pulse energy resulting from the decreased pulse repetition rate. It can be also seen that the output power and pulse energy are higher for SA with larger IT as it has a lower insertion loss. The maximum output power of 337.38 mW and pulse energy of 5.64 μJ were obtained at 2970.5 nm and 2991.5 nm by employing the Fe^{2+}:ZnSe SA with IT of 89%. Figure 4(c) shows the relative slope efficiencies as a function of tuning wavelength. Similar to the variations of output powers, their slope efficiencies coherently increase initially to the maximum at ~2970.5 nm and then decrease with tuning wavelength. At ~2970.5 nm, the maximum slope efficiencies (optical-to-optical efficiencies) were calculated to be 9.02% (8.01%), 10.8% (9.58%) and 11.44% (10.16%) with respect to the ITs of 69%, 79% and 89%, respectively, indicating increasing IT benefits to the improvement of the slope efficiency. Note that the efficiencies are higher than the level in previous report [21] mainly owing to the use of anti-reflection coating of the lens and Fe^{2+}:ZnSe crystal and enough pump absorption.

3. Discussion

In this section, further performance optimizations on the passively Q-switched pulses in terms of pulse duration, repetition rate and tunable range were discussed. Also, the relative analysis on how to achieve mode locking was given.

In our experiment, the shortest pulse duration of 1.23 μs was achieved utilizing 69% IT Fe^{2+}:ZnSe crystal at the short tuning edge of 2919.1 nm. Note that this pulse duration was longer than those demonstrated in Ref [20, 21]. mainly due to the use of longer gain fiber as a result of lower ions dopant concentration. It is well known that the limited pulse duration of a fixed Q-switched laser could be roughly estimated according to the following formula [27]:

$$\tau_p = 1.76 \frac{2T_R}{\Delta R}, \tag{1}$$

where τ_p is the limited duration of Q-switched pulse, T_R and ΔR are cavity round-trip time and modulation depth of the SA. Note that the formula is only valid when SA operates at the fully saturated state i.e., the pulse duration does not depend noticeably on the further increased pump power. Although the specific limited pulse duration in our experiment cannot be estimated considering the absent measurement of modulation depth of the Fe^{2+}:ZnSe crystal due to lack of suitable 3 μm high peak power pulsed laser source, the pulse narrowing methods could be obtained according to the above formula. Obviously, decreasing cavity

#241509 Received 21 May 2015; revised 17 Jul 2015; accepted 29 Jul 2015; published 17 Aug 2015

length and increasing modulation depth of the SA are effective ways to narrow pulse. In our case, the 7 m length Ho^{3+}-doped ZBLAN fiber in comparison to 50 cm free-space alignment length dominated in the total cavity length. Thus, decreasing the fiber length could effectively narrow the Q-switched pulses, however, it may lead to the weakened pulse power and energy as a result of the reduced total gain. In this view, a shorter fiber with a relatively larger gain is more favored by increasing the Ho^{3+} dopant concentration or launching the pump directly into the fiber core. Besides, increasing the modulation depth of Fe^{2+}:ZnSe crystal by increasing Fe^{2+} ions dopant concentration or blue-shifting the operation wavelength would be also beneficial for narrowing the Q-switched pulses. Although the above methods of narrowing pulse duration are all at the sacrifice of output power, slope efficiency and energy, the master oscillator power amplifier (MOPA) structure could function as an alternative approach to realize the power and energy improvement. In terms of increasing the repetition rate, either increasing the Fe^{2+}:ZnSe crystal IT or blue shifting the wavelength is helpful as demonstrated in the previous experiments. Furthermore, the SA saturable optical intensity is also a critical parameter. Specifically, a lower saturable optical intensity leads to a shorter build-up time of Q-switched pulses required hence a higher repetition rate. This mechanism has been also successfully used to realize high repetition rate of up to 940 kHz Q-switching at 1.5 μm waveband which has a moderate cavity length of ~7 m [28]. To sum up, if narrow pulse duration and high repetition rate are simultaneously desired, a short high gain fiber with the blue-shifted emission wavelength and a low saturable optical intensity Fe^{2+}:ZnSe crystal are favorable. Tunable range, as another important characteristic, depends on both gain spectrum of fiber and the operation bandwidth of SA. In our case, the tunable range is mainly limited by the gain spectrum of Ho^{3+}-doped ZBLAN fiber since Fe^{2+}:ZnSe crystal possesses a large absorption bandwidth covering from ~2250 nm to ~4850 nm. Moreover, the residual Fresnel reflections from intra-cavity free-space components and even imperfect angle cleaved fiber end would also shorten the passively Q-switched tunable range. Therefore, the processes e.g., lens AR-coating, high-quality large angle cleaving, etc. are also critical.

On the other hand, it should be noticed that the mode-locking cannot be generated just by changing the position of the Fe^{2+}:ZnSe crystal with respect to two plano-covex CaF_2 lens. In order to obtain CW mode locking, the following formula must be satisfied [29]:

$$E_p{}^2 > E_{sat,g} E_{sat,a} \Delta R = F_{sat,g} A_g F_{sat,a} A_a \Delta R = E_{p,t}, \tag{2}$$

where E_p is the intra-cavity pulse energy, $F_{sat,g}$ and $F_{sat,a}$ are the saturable influence of the SA and gain medium, respectively, A_g and A_a are the effective beam areas inside the gain fiber and onto the SA, respectively. ΔR is the modulation depth of the SA. Thus $E_{p,t}$ is defined as the energy threshold. The absent mode locking manifests the above energy threshold was not reached in this case. Although the Fe^{2+}:ZnSe crystal (89% IT) with a moderately low ΔR has been employed while placed at the focus of the confocal scheme (i.e., minimized A_a) to lower the energy threshold, the relatively low intra-cavity pulse energy E_p mainly resulting from low slope efficiency, large insertion loss of components and low reflection of output coupler make the above formula hard to be satisfied. In order to achieve mode locking, a high-reflection output coupler e.g., specifically designed dichroic mirror, fiber Bragg grating and AR-coated intra-cavity free-space components are recommended.

4. Conclusion

We have demonstrated a wavelength tunable passively Q-switched Ho^{3+}-doped ZBLAN fiber laser by using a Fe^{2+}:ZnSe crystal as SA and a plane-ruled grating as the wavelength selector. The maximum wavelength tuning range of stable Q-switching was over 85 nm and the output linewidth was ~1 nm. It is concluded that the pulse duration increases and the repetition rate decreases with wavelength, and lower IT benefits to narrowing pulse duration while higher IT will improve the repetition rate, pulse energy and average power. The shortest pulse duration

#241509 Received 21 May 2015; revised 17 Jul 2015; accepted 29 Jul 2015; published 17 Aug 2015

of 1.23 μs was achieved by using Fe^{2+}:ZnSe crystal with IT of 69% at the short wavelength edge of available tuning range. The maximum output power of 337.38 mW and pulse energy of 5.64 μJ were achieved at 2970.5 nm and 2991.5 nm, respectively using 89% IT Fe^{2+}:ZnSe crystal. Moreover, it is worth noting that further broadening of tuning range within the gain bandwidth (typical 2.75~3.05 μm) is expected if the residual Fresnel reflections from all intra-cavity components can be further decreased. However, larger scale wavelength tuning should explore new transitions, e.g., $^4F_{9/2} \rightarrow {}^4I_{9/2}$ transition of Er^{3+}-doped ZBLAN fiber with ~700 nm emission bandwidth ranging from ~3200 nm to ~3900 nm [11].

Acknowledgments

This work was supported by National Nature Science Foundation of China (NSFC) (61377042, 61435003 and 61378028); Program for New Century Excellent Talents in University of Ministry of Education of China (NCET-13-0094); Fundamental Research Funds for the Central Universities (ZYGX2013J058); Open Fund of Medical Optical Key Laboratory of Jiangsu Province (JKLMO201403); Open Fund of State Key Laboratory of Advanced Optical Communication Systems and Networks (2015GZKF004); Open Found of Key Laboratory of High Energy Laser Science and Technology, CAEP (2013005580).